

Supplemental Figures

Figure S1. Evaluation of binding capacity of unmodified (A) and C18-supplemented (B) Stage-TipsTM.

Figure S2. Efficiency and reproducibility of micro-bRPLC fractionation of alpha-crystallin peptides.

Figure S3. Increase in numbers of distinct identified peptides (filled bars) and protein spectral counts (open bars) for micro-bRPLC-fractionation combined with LC-MS/MS compared to single-dimension LC-MS/MS analysis of unfractionated of colon tumor peptide mixtures. Values are for 15 representative quantifiable proteins in both analysis platforms.

Figure S4. Pairwise scatter plots and Spearman correlation coefficient (r) for average spectral counts per protein acquired from analyses of three replicate cultures of 11-18 and 11-18R cells with either 20 μ g and 5 μ g inputs.

Figure S5. Comparison of the abundance ratio for 16 proteins in 11-18 vs. 11-18R cells from analyses of either 20 μ g or 5 μ g cell protein.

Figure S6. Reproducibility of 4-plex iTRAQ quantitation for analysis of two replicate cultures of 11-18 and 11-18R cells.

Figure S7. Relative iTRAQ reporter ion ratios for representative peptides corresponding to ACTIN (A), which is equally expressed in 11-18 vs 11-18R cells and ALDH3A1 (B), MVP (C) and S100P (D), which are significantly decreased in 11-18R.

Figure S8. Efficient and reproducible fractionation of PTK peptides in 20 μ g 11-18 cell by micro-bRPLC.

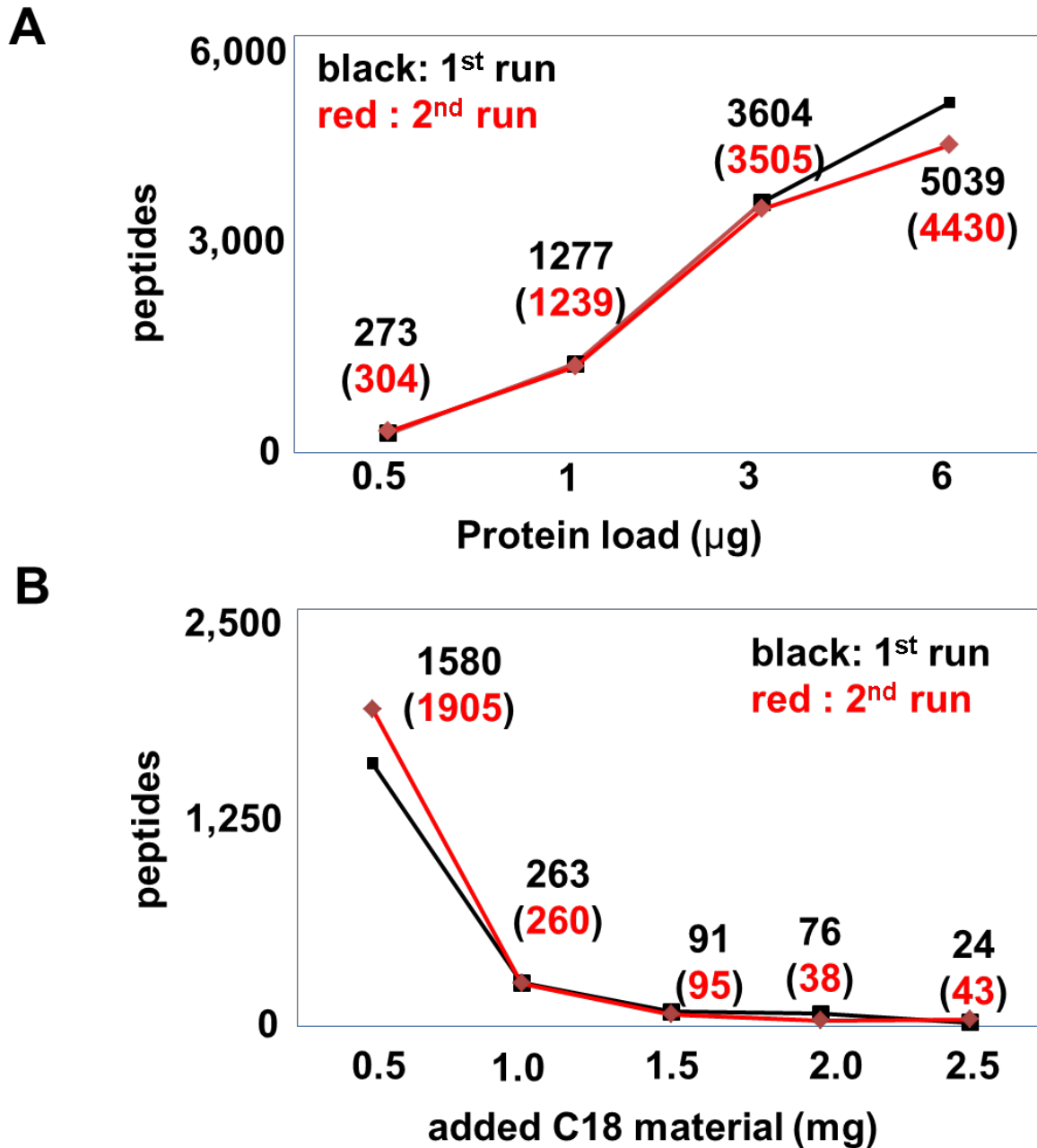


Figure S1. Evaluation of binding capacity of unmodified (A) and C18-supplemented (B) Stage-TipsTM. (A) Colon tumor protein digests at the indicated amounts were loaded on unmodified Stage Tips and the flow-through fraction was collected and analyzed by data-dependent shotgun LC-MS/MS. Digest loads above 0.5 µg exceeded the column capacity. (B) Increasing amounts of C18 material were added to Stage-TipTM columns and 20 µg colon tumor digest was loaded and the flow through fraction was analyzed by LC-MS/MS. Addition of 1.5 mg C18 was sufficient to reduce flow through peptide elution to background levels.

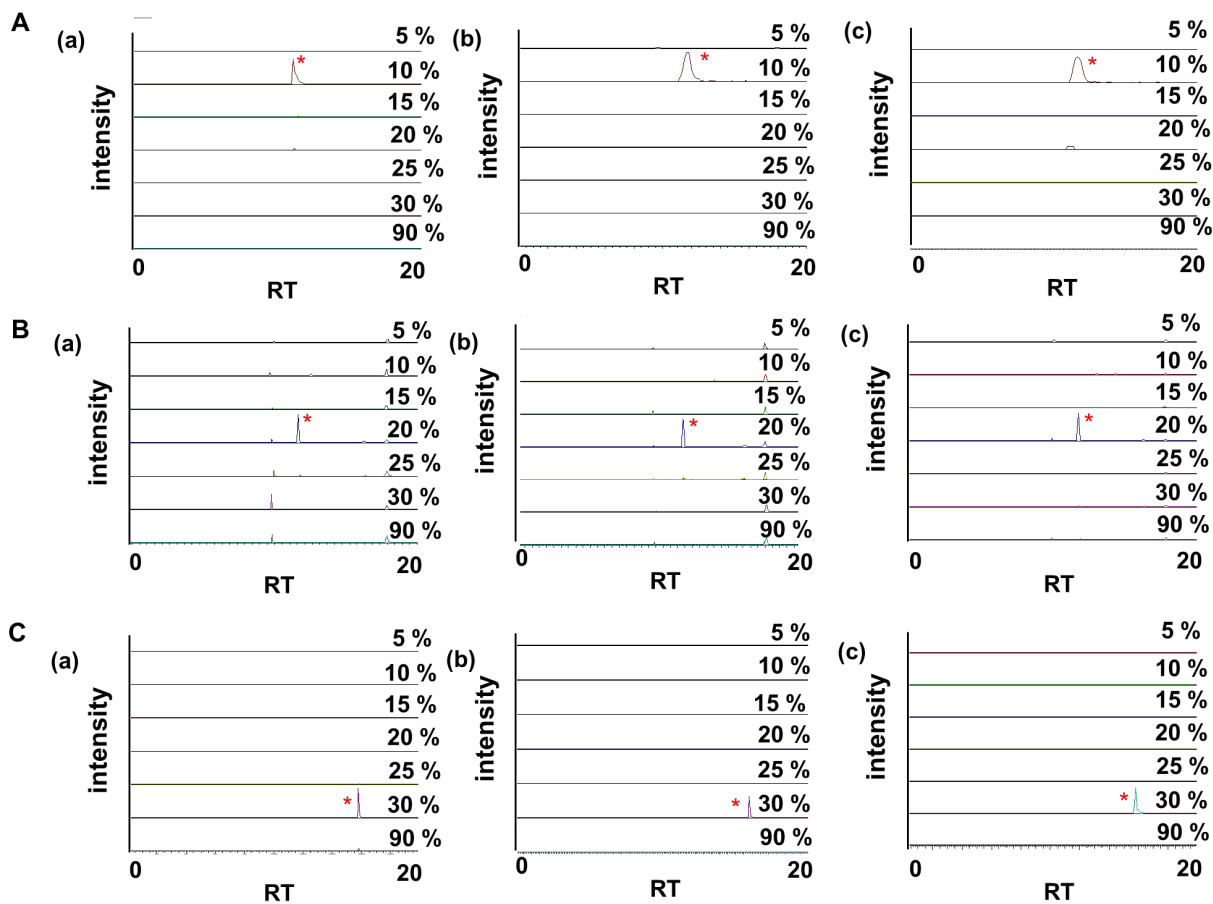


Figure S2. Efficiency and reproducibility of micro-brPLC fractionation of alpha-crystallin peptides. Three aliquots (2 μ g) alpha-crystallin, were digested and fractionated by micro-brPLC (7 fractions) and 10 % of each fraction was analyzed by LC-MS/MS. MS1 data were used to generate extracted ion chromatograms (XIC) for alpha-crystallin peptides HEERQDEHGFISREFHR (m/z 442.6150, 5+) (A), VKVLGDVIEVHGKHEER (m/z 486.7725, 4+) (B), and M(ac)DIAIQHPWFKR (m/z 528.6104, 3+) in three replicate runs (a-c) Asterisks mark the retention of the target peptides.

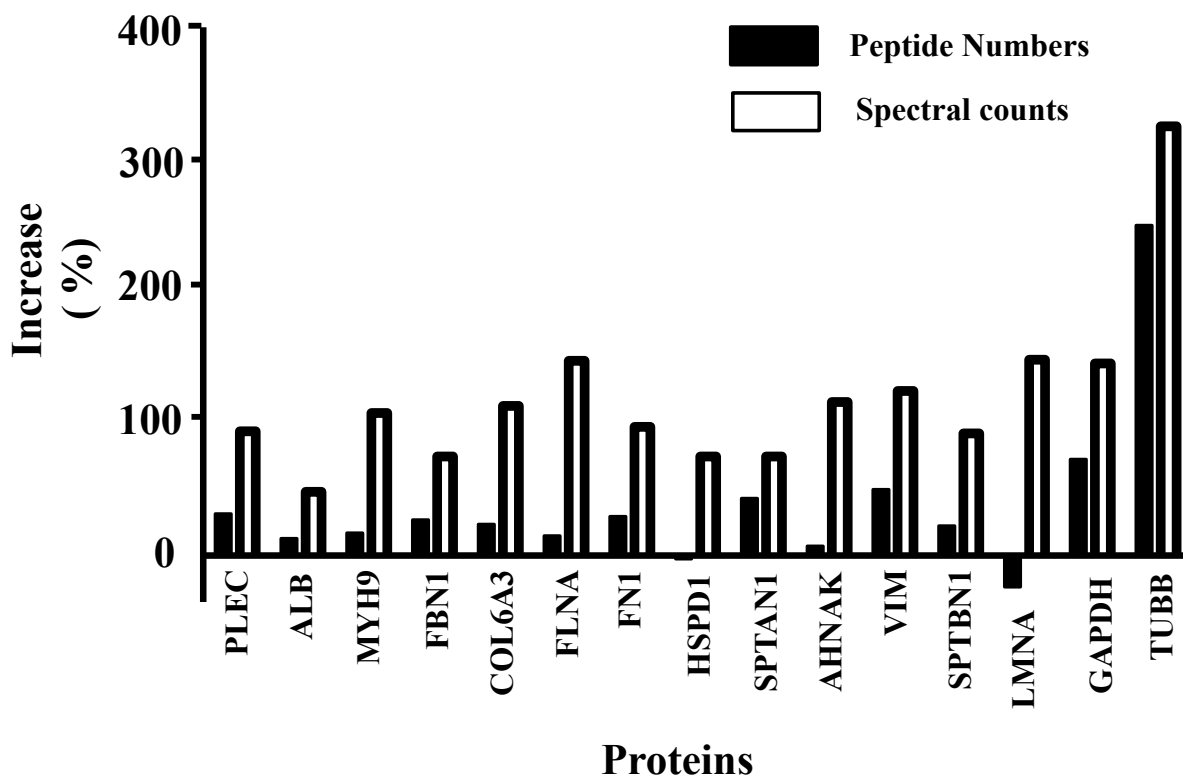


Figure S3. Increase in numbers of distinct identified peptides (filled bars) and protein spectral counts (open bars) for micro-bRPLC-fractionation combined with LC-MS/MS compared to single-dimension LC-MS/MS analysis of unfractionated of colon tumor peptide mixtures. Values are for 15 representative quantifiable proteins in both analysis platforms.

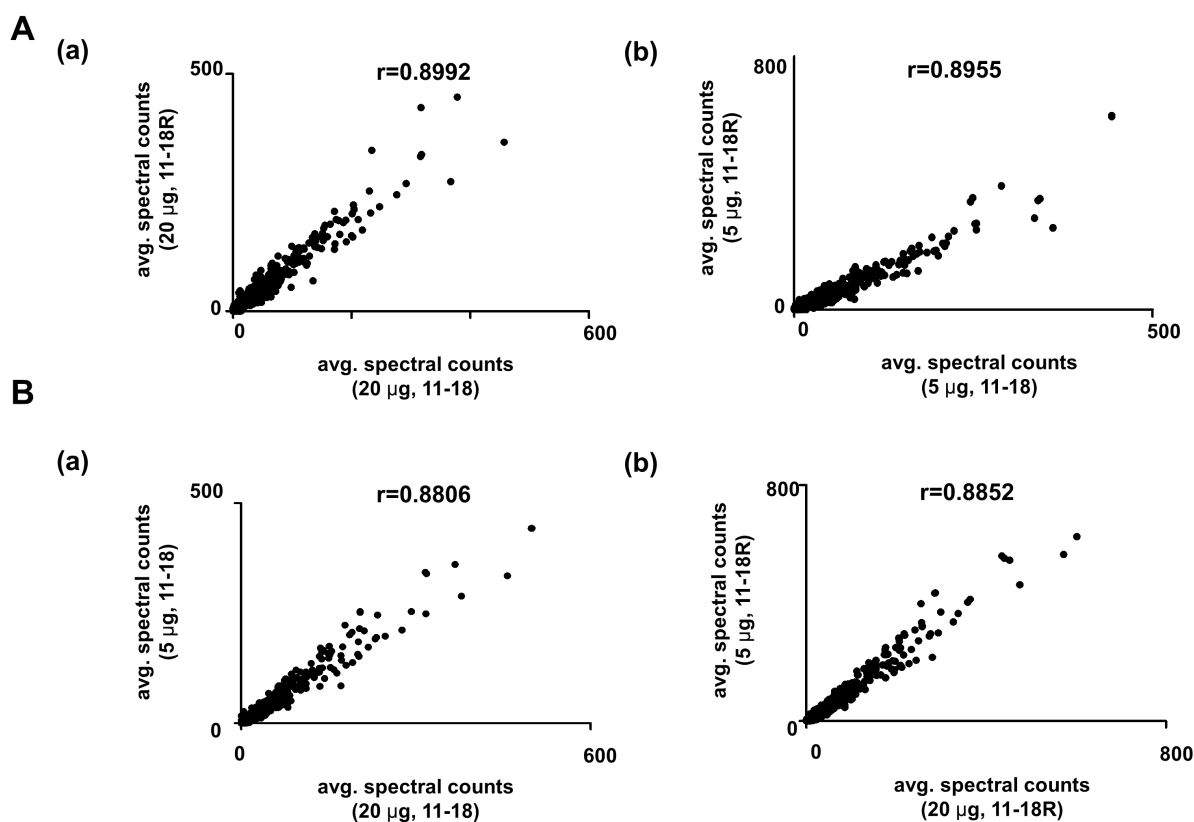


Figure S4. Pairwise scatter plots and Spearman correlation coefficient (r) for average spectral counts per protein acquired from analyses of three replicate cultures of 11-18 and 11-18R cells with either 20 μg and 5 μg inputs. (A) Spearman correlation for 11-18 versus 11-18R for 20 μg (a) and 5 μg (b) inputs. (B) Spearman correlation for 20 μg versus 5 μg inputs for 11-18 (a) and 11-18R (b). Either 20 μg or 5 μg protein from 11-18 and 11-18R cells were digested and subjected to micro-bRPLC fractionation (7 fractions). A total of 5 μg protein digest was loaded on-column for LC-MS/MS (25% of 20 μg samples and 100 % of 5 μg samples).

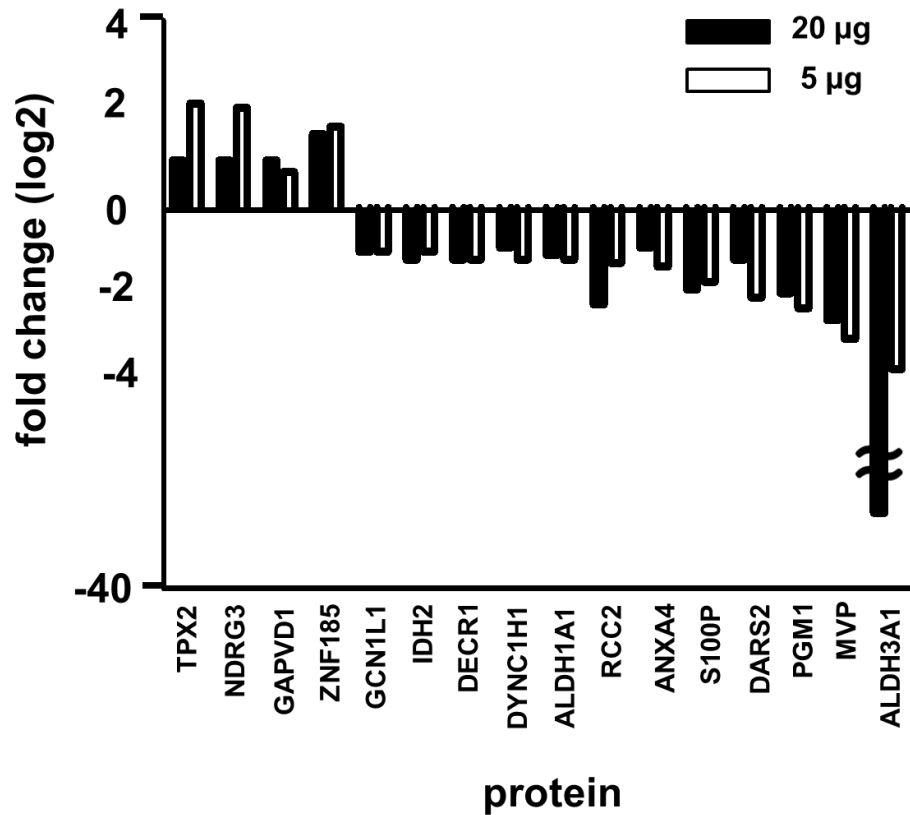


Figure S5. Comparison of the abundance ratio for 16 proteins in 11-18 vs. 11-18R cells from analyses of either 20 µg or 5 µg cell protein. Digests were fractionated by micro-bRPLC (7 fractions). A total of 5 µg protein digest was loaded on-column for LC-MS/MS (25% of 20 µg samples and 100 % of 5 µg samples). The abundance ratio for each protein was calculated from the mean spectral counts from data-dependent LC-MS/MS analyses.

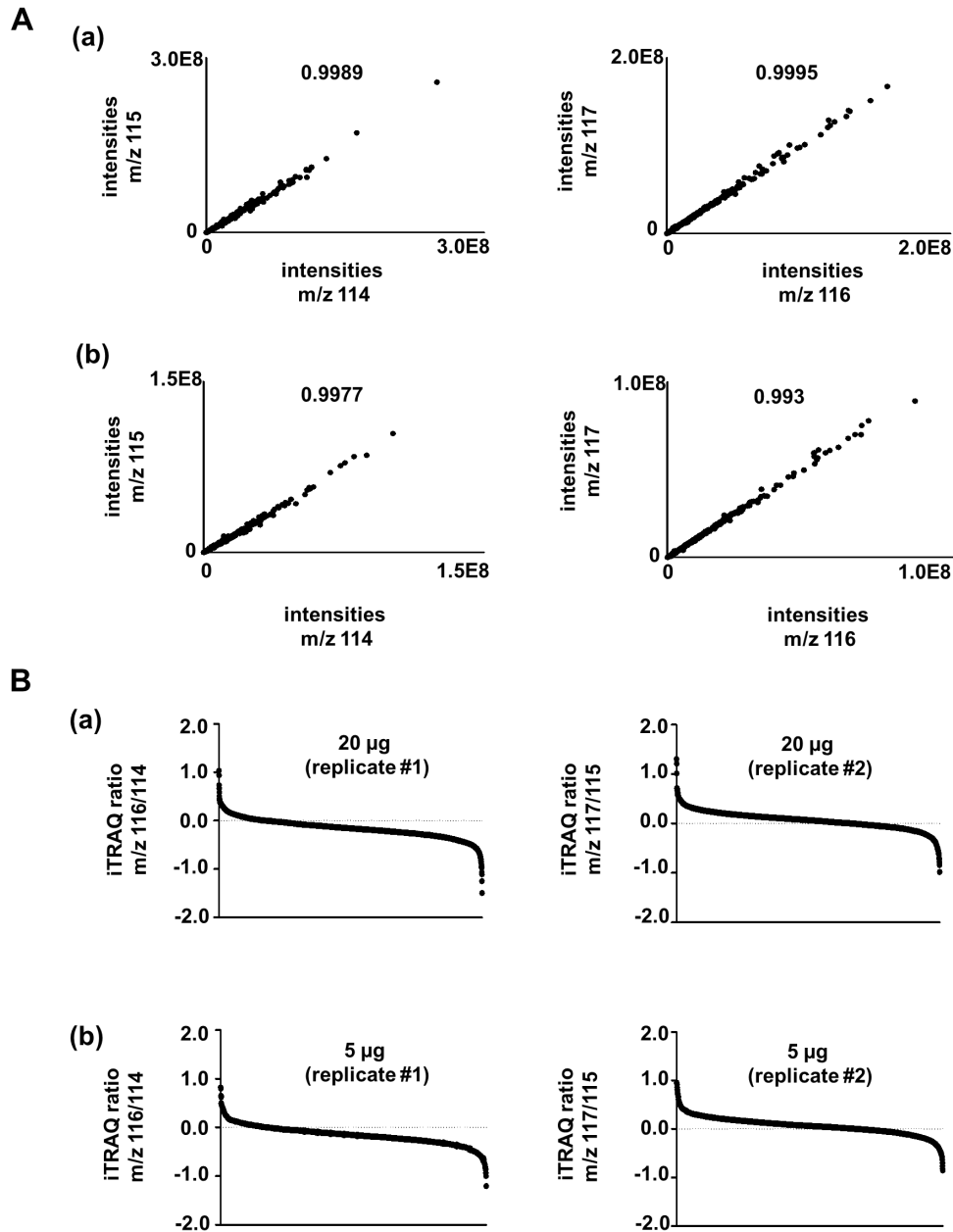


Figure S6. Reproducibility of 4-plex iTRAQ quantitation for analysis of two replicate cultures of 11-18 and 11-18R cells. Digests from two replicate cultures of each cell line were labeled with 4-plex iTRAQ (114; 11-18, 115; 11-18', 116; 11-18R, 117; 11-18R') and mixed in equal proportions. Normalized reporter ion intensities were summed for all peptides for each protein detected in both replicates. (A) iTRAQ reporter ion intensities obtained from 2 biological replicates were used for pairwise scatter plot and Spearman correlation. Both 20 µg (a) and 5 µg (b) sample loads were fractionated by micro-bRPLC (7 fractions). (B) Distribution of global iTRAQ ratio between 11-18 and 11-18R quantified with 4-plex iTRAQ for 20 µg (a) and 5 µg

(b).

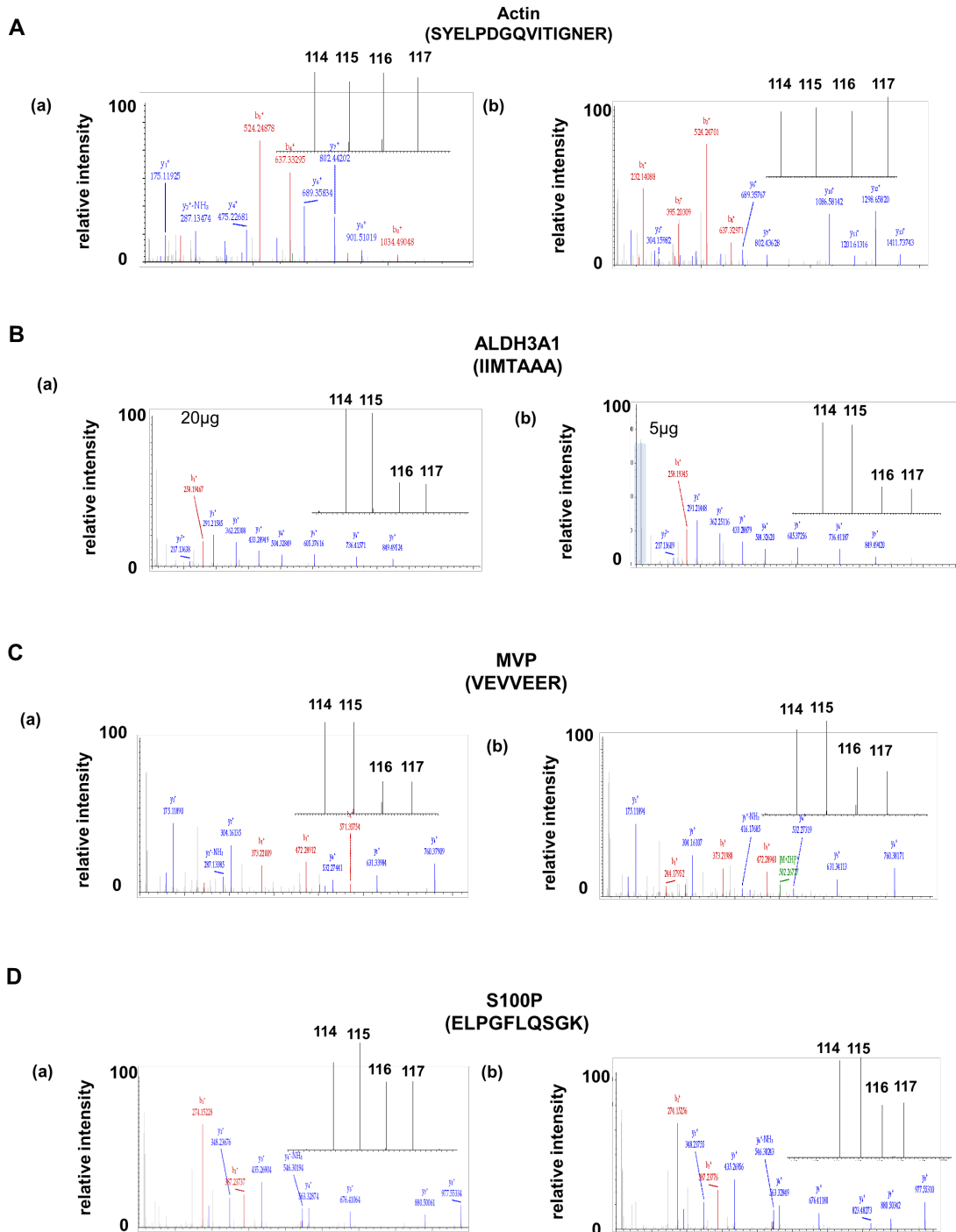


Figure S7. Relative iTRAQ reporter ion ratios for representative peptides corresponding to ACTIN (A), which is equally expressed in 11-18 vs 11-18R cells and ALDH3A1 (B), MVP (C) and S100P (D), which are significantly decreased in 11-18R. Analyses were done with micro-bRPLC fractionation of 20 µg (a) and 5 µg (b) digests.

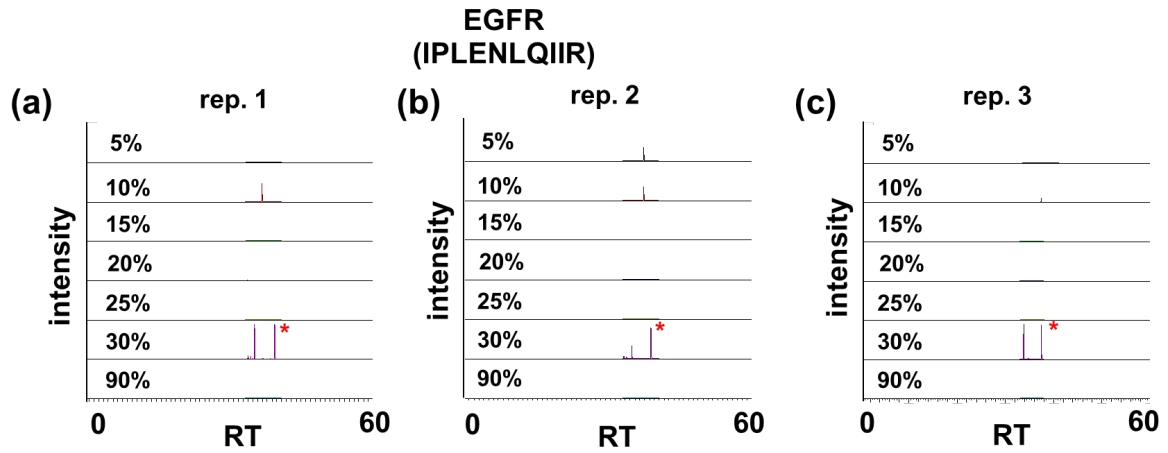
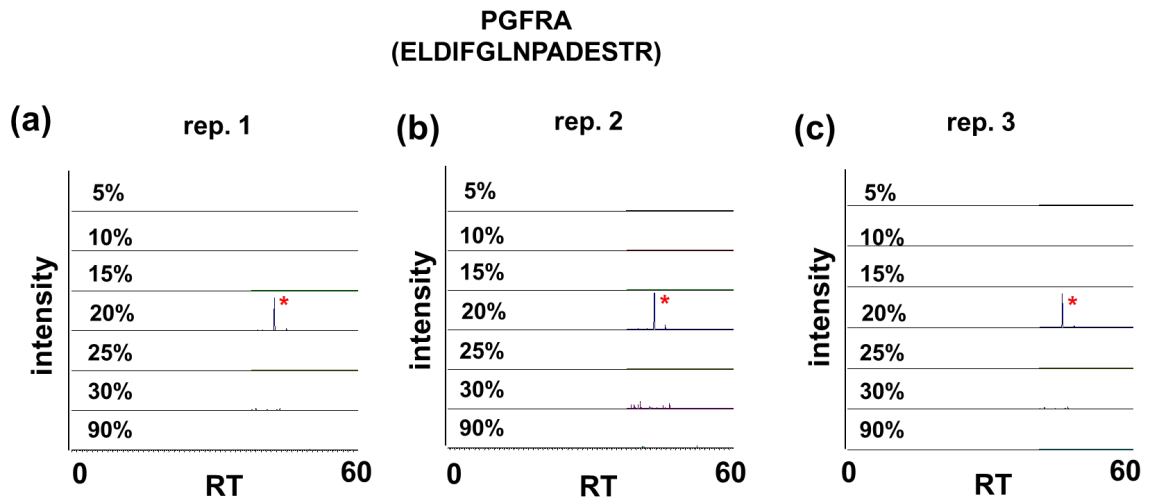
A**B**

Figure S8. Efficient and reproducible fractionation of PTK peptides in 20 μg 11-18 cell by micro-brPLC. Digests (20 μg) from three replicate cultures of 11-18 cells were fractionated by micro-brPLC (7 fractions). One fourth of each fraction was analyzed on the Orbitrap Elite instrument with SIM acquisition targeted to the peptides IPLLENLQIIR (from EGFR) (precursor m/z 604.8717, charge 2+) and ELDIFGLNPADESTR (from PDGFRA) (precursor m/z 838.9099, charge Y+). Elution of the peptide in micro-brPLC fractions is monitored by the y_7 fragment ion for IPLLENLQIIR (m/z 885.5152) (A) and by the y_7 fragment ion (m/z 775.3581) of ELDIFGLNPADESTR (B). Asterisks mark peaks for target peptides.